JOURNAL OF MATERIALS SCIENCE **32** (1997) 5945–5953

Fabrication methods for auxetic foams

N. CHAN
Institute of Aeronautics and Astronautics, National Cheng Kung University, Tainan, Taiwan 70101
K. E. EVANS
School of Engineering, Harrison Building, University of Exeter, Exeter EX4 4QF, UK

Auxetic materials have a negative Poisson's ratio, that is, they expand laterally when stretched longitudinally. Negative Poisson's ratio is an unusual property that affects many of the mechanical properties of the material, such as indentation resistance, compression, shear stiffness, and certain aspects of the dynamic performance. The unusual mechanical properties of auxetic foams are attributed to the deformation characteristics of re-entrant microstructures. One way of obtaining negative Poisson's ratio is by using a re-entrant cell structure. Auxetic foam was fabricated from a conventional polymeric foam. The fabrication method for making both small and large auxetic foam specimens is described.

1. Introduction

Materials often have a positive Poisson's ratio in nature [1]; when stretched, the material becomes thinner. Recently, synthetic materials have been processed that exhibit a negative Poisson's ratio, becoming fatter when stretched [2–7]. Such materials can have improved mechanical properties, such as enhanced shear moduli, indentation resistance and fracture toughness [2, 7–10]. All these materials exhibit a negative Poisson's ratio as a result of microstructures, or geometric units, that are at least tens of micrometres in size [5, 6, 11]. By altering the geometry of the repeat unit, Poisson's ratio can be varied to produce positive or negative values with mechanical properties that are either isotropic or anisotropic [12].

One way of obtaining negative Poisson's ratio is by using a re-entrant cell structure. Various features of the re-entrant cell shape can be controlled by processing techniques. In 1987, Lakes [2] converted an open-cell polymeric foam into an auxetic foam with a Poisson's ratio of -0.7, and developed the fabrication method for making a small auxetic foam specimen of dimensions 22 mm × 22 mm × 125 mm. The method used involved four stages: compression, heating, cooling and relaxation.

To transform a conventional flexible foam into an auxetic one using this method requires that the foam is compressed simultaneously in three dimensions to force the cell ribs to buckle. This produces a re-entrant structure which is then heated to its softening temperature to preserve the new configuration. Different types of polymeric foam (e.g. open or closed-cell) and differing densities of conventional foams require different heating times and temperatures. The conventional foams used in this work are listed in the Table I. The process used by Lakes is a one-stage compression [3] and has several problems. An auxetic foam produced in this way may exhibit long-term instability, with the material reverting to its original structure. The one-stage compression also promotes severe surface creasing. To improve the quality of the auxetic product, and to fabricate larger specimens the process was developed as described below.

2. Fabricating small auxetic polymeric foam specimens

2.1. General fabrication procedure

All the foam specimens used in this work were cut to size using a Burgess band saw fitted with a knife blade. This enabled accurate rectangular blocks to be cut with smooth faces. As a result of the foam being flexible and having a very low Young's modulus it can easily be squeezed into a small rectangular mould to achieve a three-dimensional compression. The starting point for the investigation was the method published by Friis *et al.* [3], described below.

A Gallenkamp BS oven was pre-heated to 200 °C. Next, a square section aluminium tube (e.g. with inner dimensions: 25.4 mm × 25.4 mm × 80 mm) was used as a mould for the foam which was cut oversize (38 mm × 38 mm × 110 mm in the case of the open-cell polyether urethane foam). The inner walls of the mould were then treated with a general purpose lubricant (WD 40) to aid in the insertion of the foam. At this point the foam can be inserted into the tube with the aid of a spatula to help eliminate surface wrinkles. This procedure gives compression in two transverse directions. Two end-plates made of aluminium (dimensions 1.5 mm × 25.4 mm × 25.4 mm) can then be used to block the ends of the mould, so that the foam is compressed in the third, longitudinal direction as shown in Fig. 1. The compressed foam with the buckled cell ribs was then placed in the oven at 200 °C for 8 min to "set" the new configuration. The heating time is very critical because the transformation

0022–2461 © *1997 Chapman & Hall*

TABLE I Specification of materials used, e.g. types, suppliers, densities. ppi = pores per inch

Type	Abbreviated name	Supplier	Density (kg m^{-3})
60ppi closed-cell polyester urethane foam	PECC	Caligen, UK	37.9 ± 2.1
60ppi reticulated polyester urethane foam	PECO	Caligen, UK	33.7 ± 1.3
10ppi open-cell polyether urethane foam	10CO	Reticel, Belgium	24.1 ± 3.1
30ppi open-cell polyether urethane foam	30CO	Reticel, Belgium	24.5 ± 2.7
60ppi open-cell polyether urethane foam	60CO	Reticel, Belgium	21.7 ± 1.9

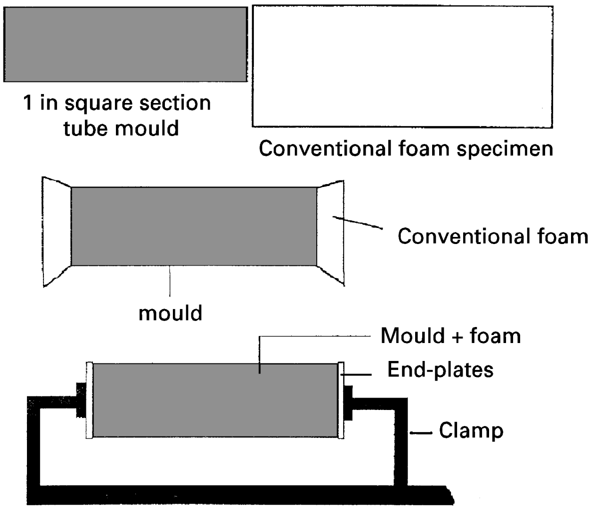

Figure 1 Schematic diagram of the fabrication of the small sized auxetic foam. The 1 in square section tube and the conventional foam specimen; Insertion of the conventional foam into the tube; Insertion of complete the assembly into the oven at 200 °C.

temperature of the foam does not reach the oven temperature. The establishment of the correct heating time is discussed later. The mould was then removed from the oven and was cooled at room temperature for 15 min. Finally, the foam was taken out of the mould by hand, and was stretched gently in each of three orthogonal directions to overcome any adhesion of the cell ribs.

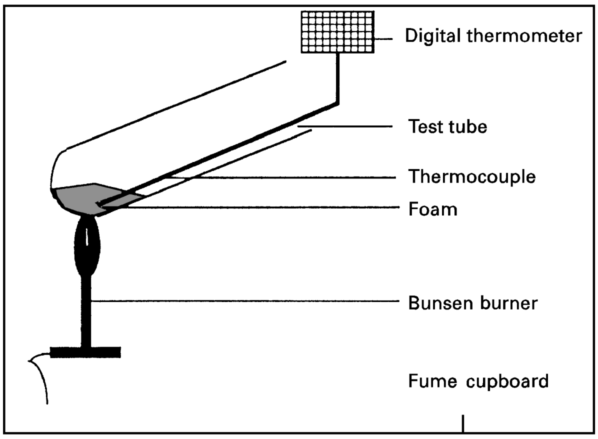

Figure 2 Schematic diagram of the examination of the heating conditions of the foam specimen.

TABLE II Investigation of the heating temperature of the foam

Type of the foam	Softening temp (°C)	Liquefaction temp. (°C)	Decomposition temp. (°C)	Oven temp (°C)
PECC	200 ± 5.6	290 ± 3.8	320 ± 6.7	200
PECO	180 ± 5.2	270 ± 4.0	300 ± 5.8	180
10CO	175 ± 7.7	240 ± 6.5	270 ± 4.2	175
30CO	175 ± 5.5	240 ± 4.3	270 ± 5.1	175
60CO	182 ± 7.3	270 ± 6.2	295 ± 4.8	182

2.2. The heating temperature

Friis *et al.* [3] carried out their work at an oven temperature of 200 °C. However, Lakes did not report how or why he decided on this temperature. As an attempt to investigate this, an experiment was performed to determine the transformation temperature required by the foam. A small specimen of foam was placed inside a test tube, and heated using a Bunsen burner. A thermocouple was inserted in the middle of the foam to measure the temperature, and the whole procedure was carried out inside a fume cupboard as shown in Fig. 2. The foam softening temperature was recorded when the cell ribs began to collapse. Three specimens were tested for each type of foam, and the average temperature was taken. Although this method is not very accurate, it was possible to obtain estimates of the softening, liquefaction and decomposition temperatures respectively.

It was noticed that the softening temperature of PECO is around 180 °C (at this temperature, the cell ribs started to collapse), the liquefaction temperature 270 °C, and the decomposition temperature 300 °C. There appears to be no sharp melting temperature for these polymeric foams. Therefore, a suitable oven temperature for this foam may be considered to be 180 °C, which was perhaps why Friis *et al.* [3] used 200 °C as the oven temperature for their foam fabrication. As a rough guide to the conversion temperature, we suggest that this should be about 5–20 °C lower than the softening temperature, in order to maximize stress relaxation and minimize cell-rib adhesion.

The different values of softening, liquefaction and decomposition temperatures for different materials are shown in Table II.

2.3. The heating time

In addition to the heating temperature, the heating time (which determines how long the foam takes to reach its softening temperature) is another very useful factor which directly affects the fabrication result.

Under static external loading conditions, one of the remarkable influences of sustained exposure to high temperatures is to produce a permanent deformation of the strained foam. At the softening point, the stress

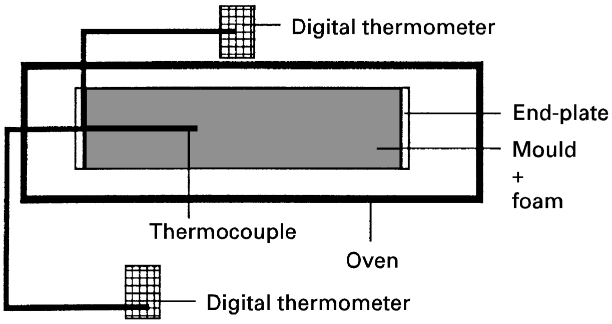

Figure 3 Schematic diagram showing the recording of the time–temperature profile for fabricating a small 1 in square sectional rectangular auxetic foam specimen (dimensions 25.4 mm × 25.4 mm × 80 mm).

of the foam relaxes to zero, therefore, a conventional foam with an outward cell structure can be converted into auxetic foam with an inward cell structure. This is similar in a sense to making a spring from iron wire.

The experiments show that if the heating time is too short, the foam cannot be "set", with the result that, after it comes out of the mould, the foam soon expands to its original size as all the internal stress has not been relaxed. If, on the other hand, the time at the softening point is too long, the foam will be either melted, so that the cell ribs stick together to form a block of dense material (this was observed with the 60ppi closed-cell polyester urethane foam, PECO); or alternatively, the foam may decompose (as in the case of the open-cell polyether urethane foams, 10CO and 30CO). In order to maximize the stress relaxation and minimize sticking and structural collapse it is very important to establish the correct heating time for the foam being used.

The time–temperature profiles for fabricating the auxetic foams have been studied. In order to determine the time–temperature profile that is required to produce an auxetic foam, the following experiment was performed. Starting with the small 1 in (25.4 mm) square tubular section we fitted one thermocouple sandwiched between the mould and the foam, and another thermocouple was inserted into the middle of the specimen (Fig. 3). The time and temperature were measured starting from the moment that the block was exposed to the high temperature in the oven and was continued after the block was removed from the oven until the temperature had fallen to well below the foam softening temperature (e.g. 30 °C). Three specimens were tested for each type of foam, the average was taken and is shown in Figs 4–8 for each of the foams tested. The time for conversion was that necessary for the centre to reach the softening temperature.

During the heating time, the specimen was left to "set" in the oven at a constant oven temperature (i.e. 200 °C). It has been found that the heating time required to transform a conventional foam into an auxetic one depends upon the type of foam being used. Table III lists the heating time required for each foam to reach its conversion temperature for a given oven temperature.

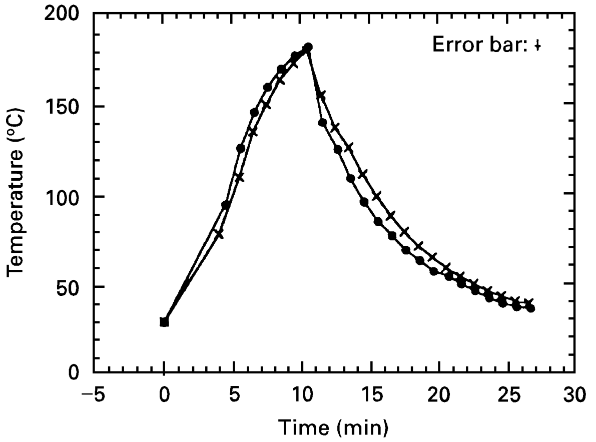

Figure 4 The time–temperature profile for making a 1 in square sectional rectangular 60ppi closed-cell polyester urethane auxetic foam (PECC) (dimensions 25.4 mm × 25.4 mm × 80 mm). (×) Temperature of foam centre; (●) temperature of foam skin.

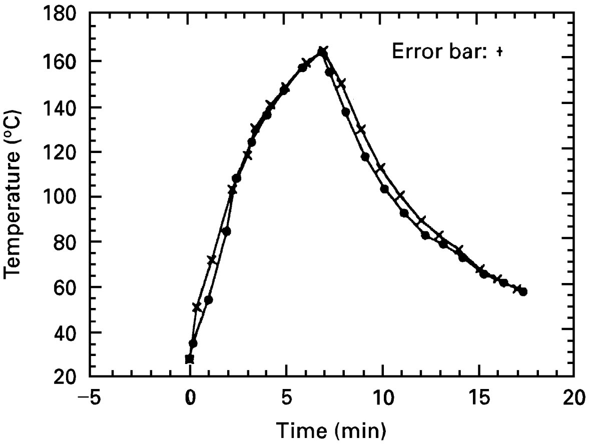

Figure 5 The time-temperature profile for making a 1 in square sectional rectangular 30ppi open-cell polyether urethane auxetic foam 30CO (dimensions 25.4 mm × 25.4 mm × 80 mm). For key, see Fig. 4.

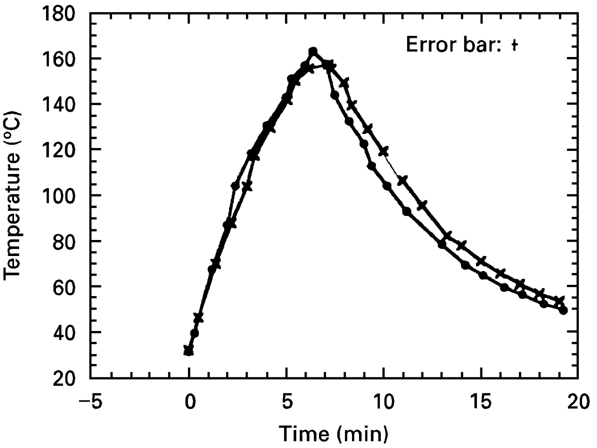

Figure 6 The time–temperature profile for making a 1 in square sectional rectangular 10ppi open-cell polyether urethane auxetic foam 10CO (dimensions 25.4 mm × 25.4 mm × 80 mm). For key, see Fig. 4.

2.4. Volumetric compression ratio

From a theoretical point of view, changing the compression ratio of a foam enables the fabrication of auxetic foams with a range of negative Poisson's

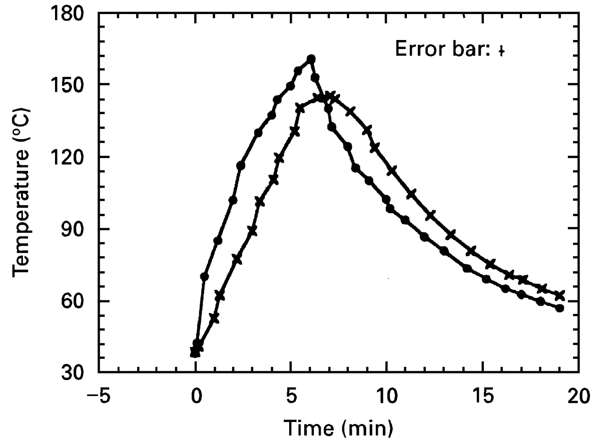

Figure 7 The time-temperature profile for making a 1 in square sectional rectangular 60ppi open-cell polyether urethane auxetic foam 60CO (dimensions 25.4 mm × 25.4 mm × 80 mm). For key, see Fig. 4.

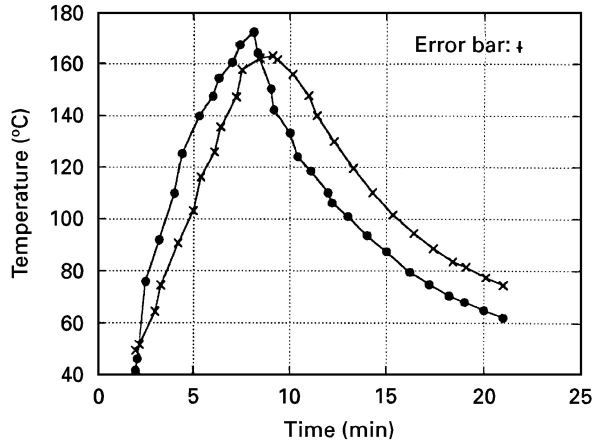

Figure 8 The time–temperature profile for making a 1 in square sectional rectangular 60ppi reticulated polyester urethane auxetic foam (PECO) (dimensions 25.4 mm × 25.4 mm × 80 mm). For key, see Fig. 4.

ratios. This determines the degree of re-entrancy of the cells. Because foams exhibit a characteristic distribution of cell sizes, the necessary effective volumetric compression ratios will vary from foam to foam to achieve a specific Poisson's ratio. In addition, anisotropy can be induced by varying the degree of compression in different directions.

In order to determine the maximum degree of compression possible for any given foam, the stress–strain curve in compression was examined (Fig. 9). The conventional foam was first cut to the dimensions $L_x \times L_y \times L_z$ (e.g. 50 mm × 50 mm × 50 mm, Fig. 10).

Figure 9 Schematic diagram for compression testing the foam.

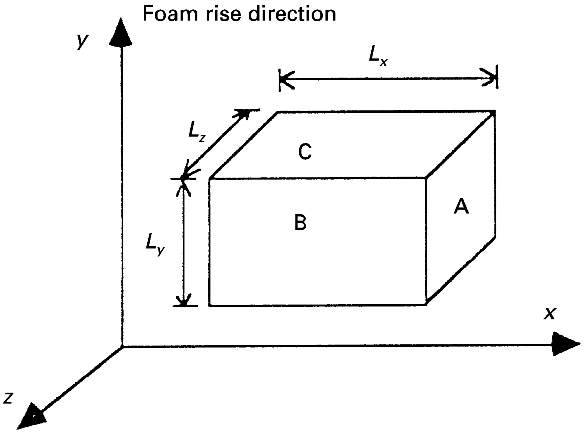

Figure 10 Schematic diagram of the three-dimensional conventional foam block.

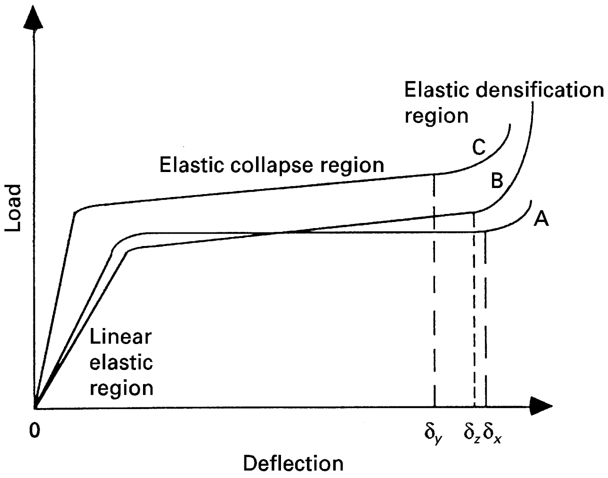

Figure 11 A schematic diagram of the load–deflection curve of the three-dimensional conventional foam. Compression along (A) in the x-direction, (B) the z-direction and (C) the y-direction.

Tests were then carried out in each of the three dimensions for every conventional foam specimen, to determine the starting point of densification shown in Fig. 11. This well-known curve [4] begins with a

TABLE III The typical time–temperature combinations for making a small auxetic foam with a volumetric compression ratio of 3.1. Note: the average error on the sample dimension is ±1 mm

Type	Heating time (min)	Oven temp. (°C)	Conversion temp. (°C)	Starting size (mm^3)	Finish size (mm^3)
10CO	6.2 ± 0.5	175 ± 2	170 ± 8	38 × 38 × 110	25.4 × 25.4 × 80
30CO	7.1 ± 0.3	175 ± 2	168 ± 6	38 × 38 × 110	25.4 × 25.4 × 80
60CO	6.0 ± 0.3	182 ± 2	175 ± 8	38 × 38 × 110	25.4 × 25.4 × 80
PECC	11 ± 0.2	200 ± 2	185 ± 6	38 × 38 × 110	25.4 × 25.4 × 80
PECO	8 ± 0.4	180 ± 2	173 ± 8	38 × 38 × 110	25.4 × 25.4 × 80

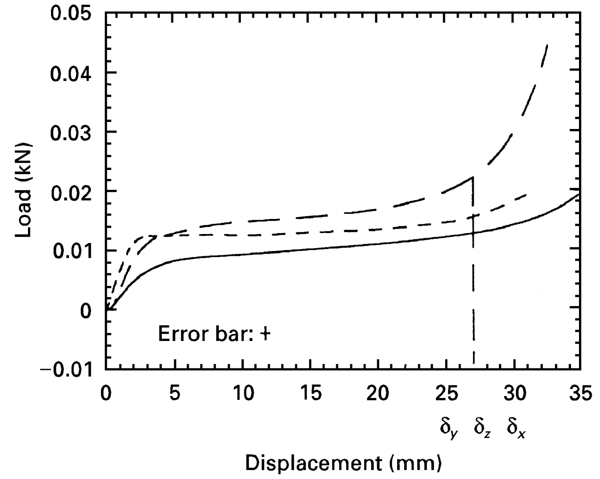

Figure 12 Compressive load–displacement curves in two orthogonal directions in the planes normal to the rise direction, Faces (——) A and (— —) B, and in the rise direction, (– – –) Face C, for the 60ppi closed cell polyester urethane foam (PECC).

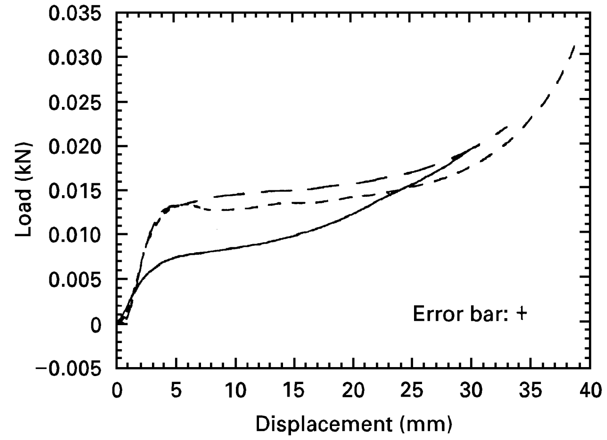

Figure 13 Compressive load–displacement curves in two orthogonal directions in the planes normal to the rise direction, Faces (– – –) A and (— —) B, and in the rise direction, (——) Face C, for the 10ppi open-cell polyether urethane foam (10CO).

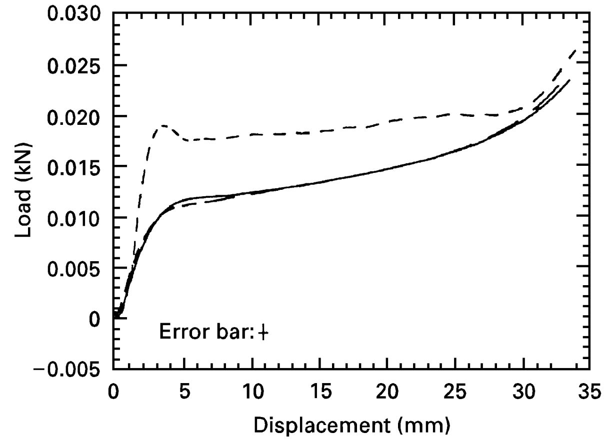

Figure 14 Compressive load–displacement curves in two orthogonal directions in the planes normal to the rise direction, Faces (——) A and (— —) B, and in the rise direction, (– – –) Face C, for the 30ppi open-cell polyether urethane foam (30CO).

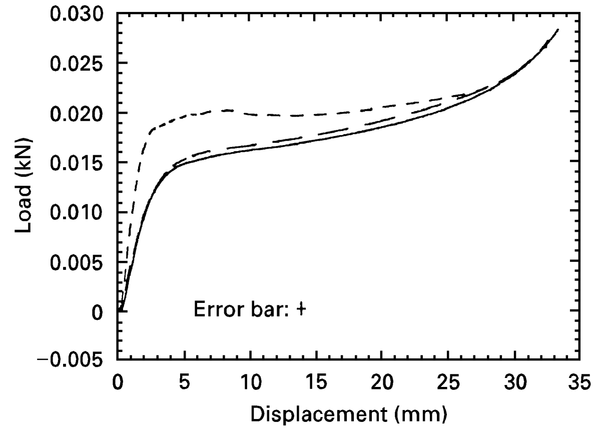

Figure 15 Compressive load–displacement curves in two orthogonal directions in the planes normal to the rise direction, Faces (——) A and (— —) B, and in the rise direction, (– – –) Face C, for the 60ppi open-cell polyether urethane foam (60CO).

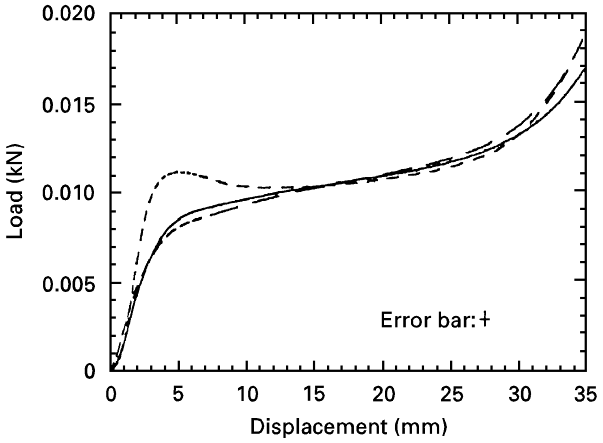

Figure 16 Compressive load–displacement curves in two orthogonal directions in the planes normal to the rise direction, Faces (——) A and (— —) B, and in the rise direction, (– – –) Face C, for the 60ppi reticulated polyester urethane foam (PECO).

linear elastic region, followed by a plateau region of buckling of cell ribs, followed by a rapid rise in stiffness again as the foam becomes fully densified. Auxetic foams were produced by compressing up to any point before densification has been reached.

The original volume for the conventional foam specimen is

$$V_0 = L_x \times L_y \times L_z \tag{1}$$

when the foam reaches the elastic densification region, the minimum volume of the compressed foam is

$$V_1 = (L_x - \delta_x) \times (L_y - \delta_y) \times (L_z - \delta_z) \tag{2}$$

where δ_y, is the maximum compression displacement of the foam rise direction, and δ_x and δ_z, are the maximum displacements of the other two directions. The maximum auxetic effect is expected when all the cell ribs have buckled and this occurs at the elastic densification displacement. Therefore, the maximum effective volumetric compression ratio is given by

$$R_c = V_0/V_1 \tag{3}$$

This should correspond to the maximum achievable negative Poisson's ratio for that foam. Experiments have shown (see Figs 12–16) that different types of foam have various maximum volumetric reductions which are due to their differing mechanical performance. The results are listed in the Table IV.

TABLE IV The theoretical maximum volumetric compression ratio of various types of foam. Note: the average error on sample dimension is ± 1 mm

Type	V_0 (mm^3)	δ_x (mm)	δ_y (mm)	δ_z (mm)	V_1 (mm^3)	R_c
10CO	52 × 52 × 51	25	25	25	27 × 27 × 26	7.276
30CO	50 × 51 × 51	30	30	30	20 × 21 × 21	14.75
60CO	50 × 51 × 50	29	29	29	21 × 22 × 21	13.4
PECC	49 × 50 × 42	27	27	27	22 × 23 × 15	13.55
PECO	50 × 51 × 51	28	28	28	22 × 23 × 23	11.17

TABLE V Various compression ratios of the 60ppi reticulated polyester urethane foams (PECO). Note: the average error on sample dimension is ± 1 mm

	Starting size (mm^3)	Final size (mm^3)	Volumetric compression ratio	Tensile Poisson's ratio, ν_{yx}
PEAO-1	38 × 38 × 100	25.4 × 25.4 × 70	3.2	-0.78 ± 0.13
PEAO-2	33 × 33 × 100	25.4 × 25.4 × 70	2.4	-0.57 ± 0.10
PEAO-3	30 × 30 × 100	25.4 × 25.4 × 70	2.0	-0.34 ± 0.04
PEAO-4	38 × 38 × 120	25.4 × 25.4 × 70	3.8	-0.82 ± 0.03
PEAO-5	25.4 × 25.4 × 100	25.4 × 25.4 × 70	1.4	$+0.1 \pm 0.03$

The following points should be noted. (1) The experiments described above have been conducted under conditions of uniaxial loading, whilst the fabrication method involves triaxial loading. As a result of this, the volumetric compression ratios found in the experimental work are smaller than that of the maximum values expected. (2) From a practical point of view, we need to give considerations to the visco-elastic behaviour of polymeric foams, especially at high temperatures.

By compressing different size starting blocks in the same mould, followed by heating, cooling and relaxation of the foams, a range of auxetic foams can be made with a variety of Poisson's ratios. The results obtained on the 60ppi polyester urethane foams (PECO) are shown in Table V, from which we can see how the Poisson's ratio varies with the compression ratio.

3. Fabricating large auxetic foam blocks

In order to fabricate larger specimens, it was necessary to develop the fabrication process further. Clearly, the force now required to compress larger blocks of foam (dimensions 300 mm × 300 mm × 100 mm) is higher. For this reason, the mould has to be strong enough to withstand this extra force. Fig. 17 shows the arrangement. Although the low moduli of the foams allows the use of a mould to achieve our purpose, it does, however, present another problem i.e., the creasing effect. This creasing effect is due to the volume of the larger block. By inspection, it is clear that the large volume reduction indicated will require large compression of the sides. Clearly, to expect to achieve this in one step without creasing the surface is unrealistic. The surface creasing is due to the non-uniform local collapse of the foam. In order to overcome this problem, a multi-stage heating and compression process method was developed, featuring a substantially smaller compression ratio for each stage, thus minimizing the risk of creasing. One stage of this approach is illustrated in Fig. 18.

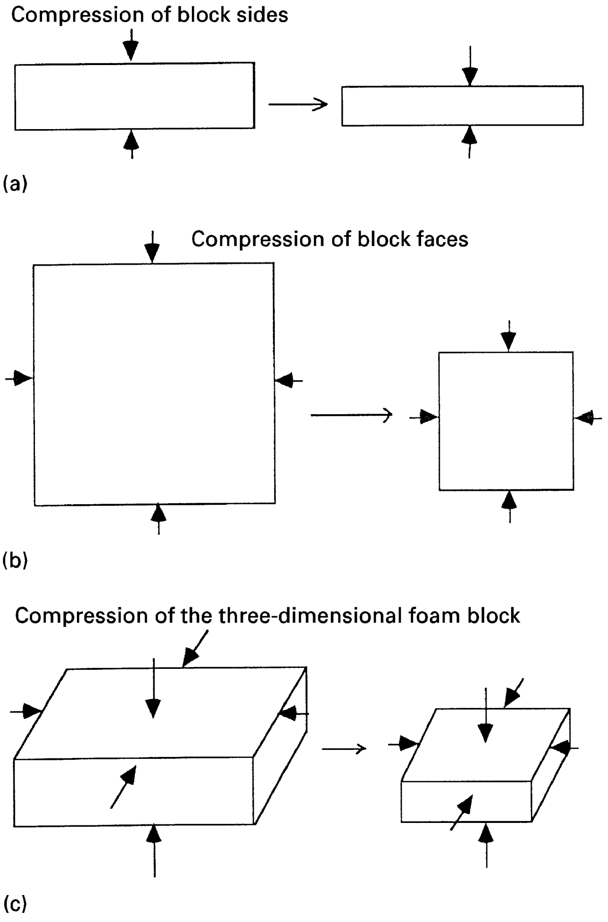

Figure 17(a–c) Schematic diagrams of the arrangement for fabricating a large auxetic foam block.

We can achieve the desired compression by carrying out the procedure in four stages. For example, if we consider the conventional foam to have the initial dimensions of 300 mm × 300 mm × 76 mm, the four stages involved in the reduction would be to first

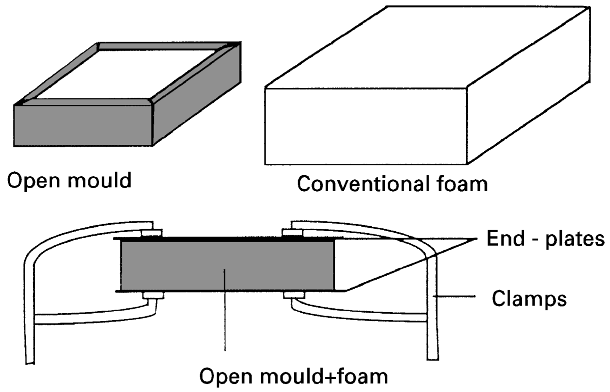

Figure 18 Schematic diagram for processing the large auxetic foam block.

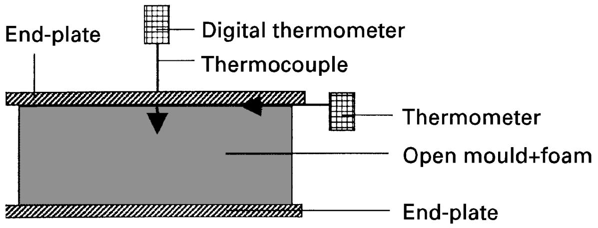

Figure 19 Schematic diagram of examining the time–temperature profile for fabricating the large auxetic foam block.

reduce its dimensions to 275 mm × 275 mm × 69.5 mm, then 250 mm × 250 mm × 63 mm, followed by 225 mm × 225 mm × 56.5 mm and then finally, 200 mm × 200 mm × 50 mm. This will achieve a total compression ratio of 3.4. The open-ended mould was made by bolting four 5 mm thick polished stainless steel plates together. The four stages require four different sized moulds for which the inner dimensions were as given above. Prior to use, the inner walls of the mould were lubricated with WD 40, so that the foam can be slid into position despite the restraining effect of the pressure-induced friction. The top and bottom pressure plates were also made of 5 mm thick polished stainless steel, and were lubricated with WD 40.

The first step in using the moulds involved squeezing the 300 mm × 300 mm × 76 mm block into place in the 275 mm × 275 mm × 69.5 mm mould by hand. The top plate was carefully manipulated into position to achieve a uniform distribution of cell pressure, to avoid surface creasing in the mould, and then it was clamped down. The whole assembly was then placed into the laboratory oven at 200 °C.

From the moment the foam was put into the preheated oven, the time and temperature of the skin and the middle of the foam specimen, were recorded (see Fig. 19). From these measurements, a plot of the time–temperature profile (Fig. 20) was produced. At

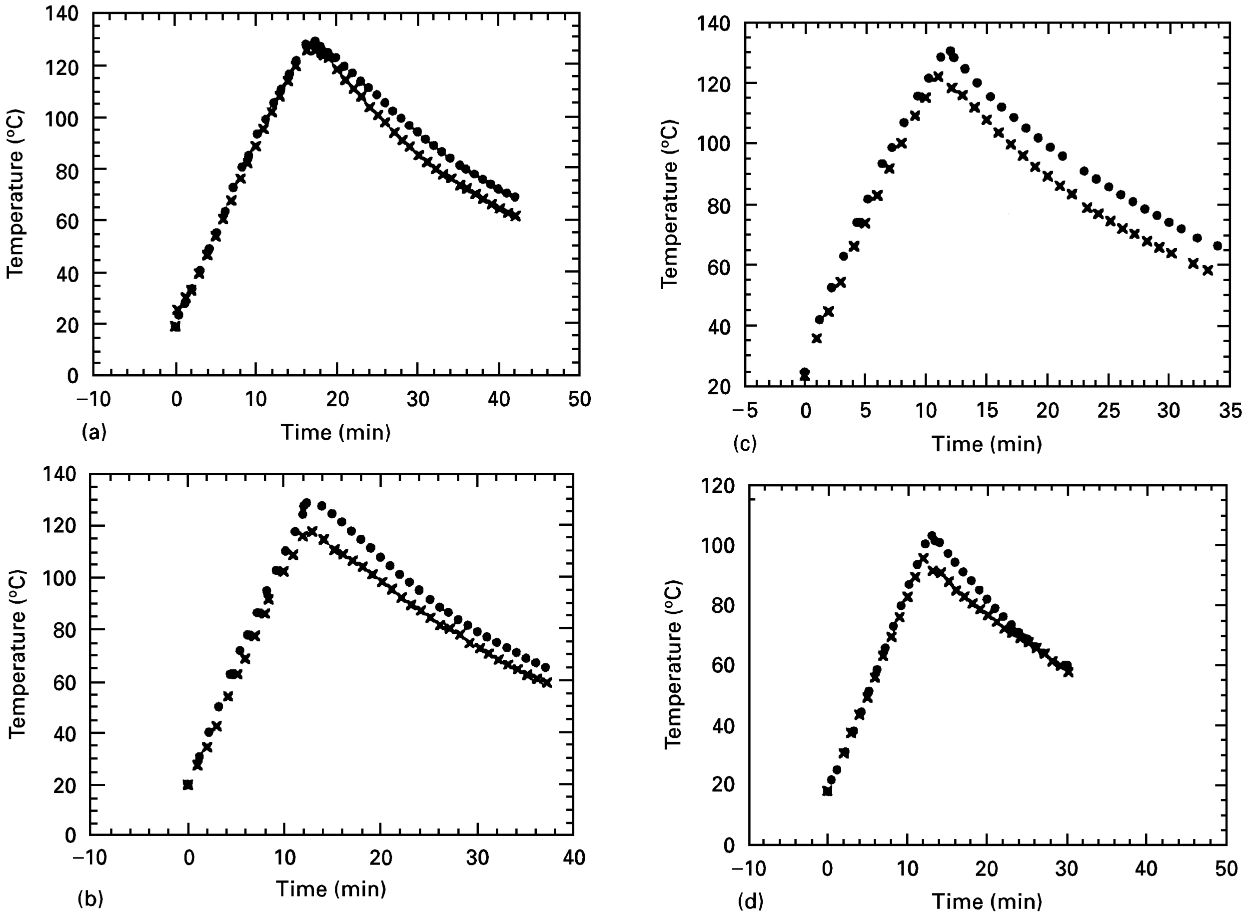

Figure 20 The time–temperature profiles of the 10ppi open-cell polyether urethane foam heated in (a) mould 1 (average error of the temperature measurements is ± 1.2 °C), (b) mould 2 (average error of the temperature measurements is ± 1.5 °C) (c) mould 3 (average error of the temperature measurements is ± 2.1 °C, (d) mould 4 (average error of the temperature measurements is ± 1.7 °C), (×) temperature of foam skin, (●) temperature of foam centre.

TABLE VI The heating time for fabricating the 10, 30, and 60ppi open-celled polyether urethane foam blocks. (Starting conventional foam dimensions: 300 mm × 300 mm × 76 mm. Final auxetic foam dimensions: 200 mm × 200 mm × 50 mm.) Note: the average error on sample dimension is ±1 mm

Type of foam	Heating time (min)				Total heating time (min)
	Mould 1	Mould 2	Mould 3	Mould 4	
10CO	17.1 ± 0.35	12 ± 0.27	12 ± 0.21	11.8 ± 0.33	52.9 ± 1.16
30CO	16.8 ± 0.23	15 ± 0.32	14.1 ± 0.28	13 ± 0.25	58.9 ± 1.08
60CO	20.8 ± 0.34	18.2 ± 0.24	16.3 ± 0.19	15.5 ± 0.21	70.8 ± 0.98

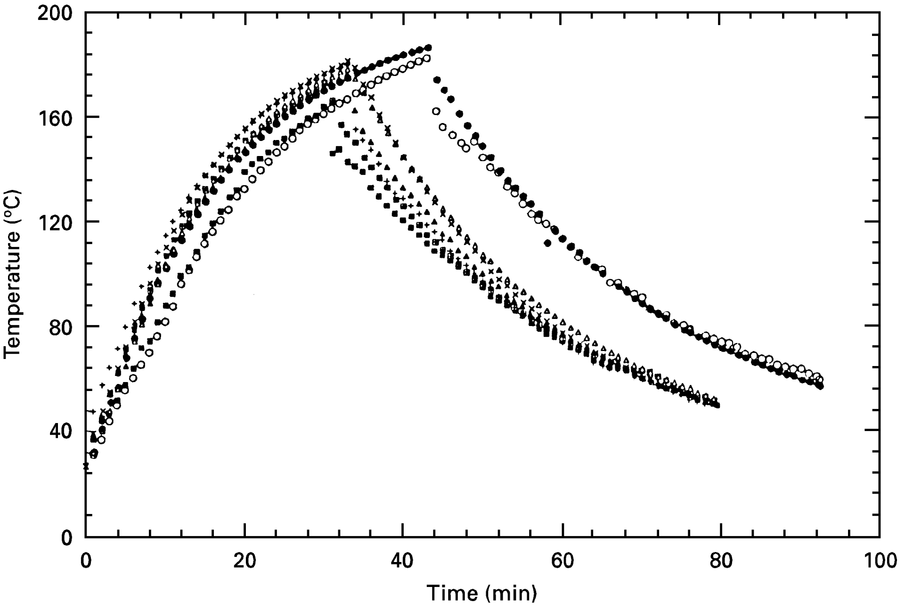

Figure 21 The time–temperature profiles for fabricating the large 60ppi polyester urethane auxetic foam block. Note: The average error of the temperature measurements is ±2.4 °C. Moulds (●, ○) 1, (■, □) 2, (△, ▲) 3 and (+, ×) 4. Temperature at (●, ■, ▲, +) skin, and (○, □, △, ×) centre.

the end of the heating time, on reaching the softening point, the specimen and mould assembly were removed from the oven and were cooled at room temperature for 2 h. Finally, the foam with a volume of 275 mm × 275 mm × 69.5 mm was taken out of the mould, and gently stretched by hand in each of the three orthogonal directions to relax the cell ribs. The temperatures used here to establish the heating time, compared with the temperatures used to convert the small specimens, are lower, because the heating time of the larger moulds is much longer than that for the single stage method.

A new time–temperature profile has to be recorded at each of the four compression stages. This is because the density of the foam is changing at each stage and therefore the time taken to reach the conversion temperature will also be changing. Similar curves were obtained for all the open-celled polyether urethane foams. The results are shown in Table VI.

The block started to cool as soon as it was removed from the oven. After allowing the specimen to cool to the room temperature, the assembly was dismantled. It was found that the final block had "set" at the reduced dimensions defined by the final mould (200 mm × 200 mm × 50 mm). The 60ppi closed-cell polyester urethane foam block (Fig. 21), was converted by the same fabrication method.

It was found that the time–temperature profiles of the foam blocks were repeatable to a high degree. As a consequence, the thermocouple was no longer required once the time–temperature profile for the foam had been established. This means that the thermocouple does not have to be used for the production runs. This avoids the introduction of surface gouges in the foam at the centre of the large faces. This method works well for the fabrication of large auxetic foam blocks. Obviously, the moulds could be made to conform to any reasonable size or shape.

4. Measurements of Poisson's ratio

It has been found that by simply changing the size of the initial conventional foam blocks, the volumetric compression ratio also changes, and a range of auxetic foams with various negative Poisson's ratio can be made. The results of varying the compression ratio to obtain different values of Poisson's ratio (measured at each stage) are shown in Tables VII–IX. Further detailed measurements of Poisson's ratio in different directions can be found elsewhere [13]. Poisson's ratios for conventional and auxetic foams can be determined in both tension and compression and they may be greater than 0.5 or less than −1 and do not violate any physical law, because the foam is not isotropic.

TABLE VII Transformation of the 10ppi open-cell polyether urethane foam blocks into a range of auxetic foams with different negative Poisson's ratios. The average error on sample dimension is ±2 mm

Starting type	Final type	Starting volume (mm^3)	Final volume (mm^3)	$\frac{L_x}{L_x - \delta_x}$ $(x = z)$	$\frac{L_y}{L_y - \delta_y}$	R_c	Tensile Poisson's ratio, ν_{yx}
10CO	100AO	300 × 300 × 100	200 × 200 × 50	1.5	2	4.5	-0.82 ± 0.05
10CO	90AO	300 × 300 × 90	200 × 200 × 50	1.5	1.8	4.05	-0.78 ± 0.04
10CO	80AO	300 × 300 × 80	200 × 200 × 50	1.5	1.6	3.6	-0.68 ± 0.02
10CO	70AO	300 × 300 × 70	200 × 200 × 50	1.5	1.4	3.15	-0.53 ± 0.01

TABLE VIII Transformation of the 30ppi open-cell polyether urethane foam blocks into a range of auxetic foams with different negative Poisson's ratios. The average error on sample dimension is ±2 mm

Starting type	Final type	Starting volume (mm^3)	Final volume (mm^3)	$\frac{L_x}{L_x - \delta_x}$ $(x = z)$	$\frac{L_y}{L_y - \delta_y}$	R_c	Tensile Poisson's ratio, ν_{yx}
30CO	100AO	300 × 300 × 100	200 × 200 × 50	1.5	2	4.5	-0.75 ± 0.10
30CO	90AO	300 × 300 × 90	200 × 200 × 50	1.5	1.8	4.05	-0.67 ± 0.11
30CO	80AO	300 × 300 × 80	200 × 200 × 50	1.5	1.6	3.6	-0.56 ± 0.02
30CO	70AO	300 × 300 × 70	200 × 200 × 50	1.5	1.4	3.15	-0.50 ± 0.03

TABLE IX Transformation of the 60ppi closed-cell polyester urethane foam blocks into a range of auxetic foams with different negative Poisson's ratios. The average error on sample dimension is ±1 mm

Starting type	Final type	Starting volume (mm^3)	Final volume (mm^3)	$\frac{L_x}{L_x - \delta_x}$ $(x = z)$	$\frac{L_y}{L_y - \delta_y}$	R_c	Tensile Poisson's ratio, ν_{yx}
PECC	PEAC-1	300 × 300 × 100	200 × 200 × 50	1.5	2	4.5	-0.68 ± 0.11
PECC	PEAC-2	300 × 300 × 90	200 × 200 × 50	1.5	1.8	4.05	-0.63 ± 0.1
PECC	PEAC-3	300 × 300 × 80	200 × 200 × 50	1.5	1.6	3.6	-0.55 ± 0.04
PECC	PEAC-4	300 × 300 × 70	200 × 200 × 50	1.5	1.4	3.15	-0.49 ± 0.03

5. Conclusion

The fabrication method for auxetic foams has been developed further. We can now not only transform the small sized conventional foam into an auxetic one, but also can produce large auxetic foam blocks. The stability of the auxetic foams has been improved by using the multi-stage method.

The processing conditions, such as the heating time, conversion temperature and volumetric compression ratios, have been examined on both small sized specimens and the larger foam blocks. Fabricating a small sized specimen requires a shorter heating time and lower compression load, whereas, fabricating the large auxetic foam block needs a much longer heating time and requires a much bigger compression force. The multi-stage processing method is preferred for such specimens.

The multi-stage processing technique, which separates the transformation process into several stages, can be used to minimize the risk of surface creasing, and therefore is a more controlled technique than the one-stage processing method, producing more homogeneous specimens.

By changing the volumetric compression ratio, different values for Poisson's ratio of the foam can be obtained. By changing the linear compression ratio in different directions, different degrees of anisotropy can be produced.

Acknowledgement

Dr N. Chan thanks the department of Materials Science and Engineering, the University of Liverpool, UK, for provision of departmental facilities during her PhD study.

References

1. L. D. LANDAU and E. M. LIFSHIITZ, "Theory of Elasticity", 2nd Edn (Pergamon, Oxford, 1970).
2. R. S. LAKES, *Science* **235** (1987) 1038.
3. E. A. FRIIS, R. S. LAKES, and J. B. PARKS, *J. Mater. Sci.* **23** (1988) 4406.
4. L. J. GIBSON and M. F. ASHBY, "Cellular Solids: Structure and Properties" (Pergamon, Oxford, 1988).
5. B. D. CADDOCK and K. E. EVANS, *J. Phys. D.* **22** (1989) 1877.
6. K. E. EVANS and B. D. CADDOCK, *J. ibid.* **22** (1989) 1883.
7. K. E. EVANS, *Chem. Ind.* **20** (1990) 654.
8. R. S. LAKES, *Adv. Mater.* **5** (1993) 293.
9. R. S. LAKES, P. ROSAKIS and A. RUINA, *J. Mater. Sci.* **28** (1993) 4667.
10. K. E. EVANS, *Endeavour* **15**(4) (1991) 170.
11. K. L. ALDERSON and K. E. EVANS, *J. Mater. Sci.* **28** (1993) 4092.
12. N. CHAN and K. E. EVANS, *J. Mater. Sci.* **32** (1997) 5725.
13. N. CHAN, PhD Thesis, University of Liverpool, 1996.

Received 16 October 1996
and accepted 1 May 1997